Structural modifications of dodecatungstophosphoric acid hexahydrate induced by temperature in the 10–358 K range. In situ high-resolution neutron powder diffraction investigation

A. Kremenovic, Anne Spasojevic - de Biré, F. Bouree, Ph. Colomban, R. Dimitrijević, M. Davidović, U.B. Mioč

Structural modifications of dodecatungstophosphoric acid hexahydrate induced by temperature in the 10–358 K range. In situ high-resolution neutron powder diffraction investigation

A. Kremenovic´ [a,b,*], A. Spasojevic´-de Bire´ [a], F. Boure´e [c], Ph. Colomban [d], R. Dimitrijevic´ [b], M. Davidovic´ [e], U.B. Miocˇ [f]

[a] Laboratoire de Structures, Proprie´te´s et Mode´lisation des Solides (SPMS), UMR 8580 du CNRS, Ecole Centrale Paris, 1 Grande Voie des Vignes, 92295 Chaˆtenay-Malabry Ce´dex, France

[b] Faculty of Mining and Geology, Department of Crystallography, University of Belgrade, Djusina 7, 11000 Belgrade, Yugoslavia

[c] Laboratoire Le´on Brillouin, (CEA–CNRS) CEA-Saclay, 91191 Gif-sur-Yvette Ce´dex, France

[d] Laboratoire de Dynamique, Interactions et Re´activite´ (LADIR), UMR 7075 du CNRS et Universite´ P. et M. Curie, 2 rue Henri Dunant, 94320 Thiais, France

[e] The Institute of Nuclear Science ‘‘Vincˇa’’, P.O. Box 522, 11001 Belgrade, Yugoslavia

[f] Faculty of Physical Chemistry, University of Belgrade, P.O. Box 550, 11000 Belgrade, Yugoslavia

Received 26 July 2001; accepted 26 April 2002

[*] Corresponding author. Faculty of Mining and Geology, Department of Crystallography, University of Belgrade, Djusina 7, 11000 Belgrad +381-11-411-747.

E-mail addresses: kremen@spms.ecp.fr, kremen@Eunet.yu (A. Kremenovic´).

Abstract

Dodecatungstophosphoric acid hexahydrate $H_3PW_{12}O_{40}6H_2O$ crystal structure has been investigated by neutron powder diffraction (NPD) at different temperatures in the 10–358 K range. A nonconvergent reversible phase transition has been noticed at about 320 K. This transition is associated with a change in dynamic equilibrium of hydrate species and partial reduction/oxidation (redox) $W^{6+}XW^{5+}$. Expressive structure changes lie in the PUO bonding inside Keggin's anion and the $H_5O^+_2$ conformational angle.

Keywords: Crystal structure; Dodecatungstophosphoric acid hexahydrate; Neutron powder diffraction; Nonconvergent phase transition; Dioxonium ion; Disorder

1. Introduction

A heteropolycompound—dodecatungstophosphoric acid $H_3PW_{12}O_{40}nH_2O$ (n-WPA), which has been known for more than a century [1], is the subject of extensive investigations focused on both: fundamental research and technological applications [2]. The applications, mainly in analytical chemistry, bio- chemistry and catalysis are connected to the high reduction/oxidation (redox) properties, high charges and high ionic weights of heteropolyions. Large heteropolytungstate ions exhibit antiviral and antitumoral properties at noncytotoxic doses in vitro and in vivo, and are potent inhibitors of cellular, bacterial and viral DNA and RNA polymerases [3–7]. Heteropolyacids and their salts have been used as heterogeneous catalysts for a number of reactions: oxidation of propylene and isobutylene to acrylic and methacrylic acids, oxidation of aromatic hydrocarbons, olefin polymerization, epoxidation [8,9].

The results of Nakamura et al. [10] defending heteropolyacids as superionic protonic conductors at room temperature have stimulated the attention for heteropoly compounds. These researches are interesting from a fundamental point of view as well as for the various possible applications [10,11]. Crystalline 12-tungstophosphoric, 12-molubdophosphoric and 12-silicophosphoric acids are excellent conductors in high hydrate state and they are electrochromic in solid state as a consequence of their redox properties [12].

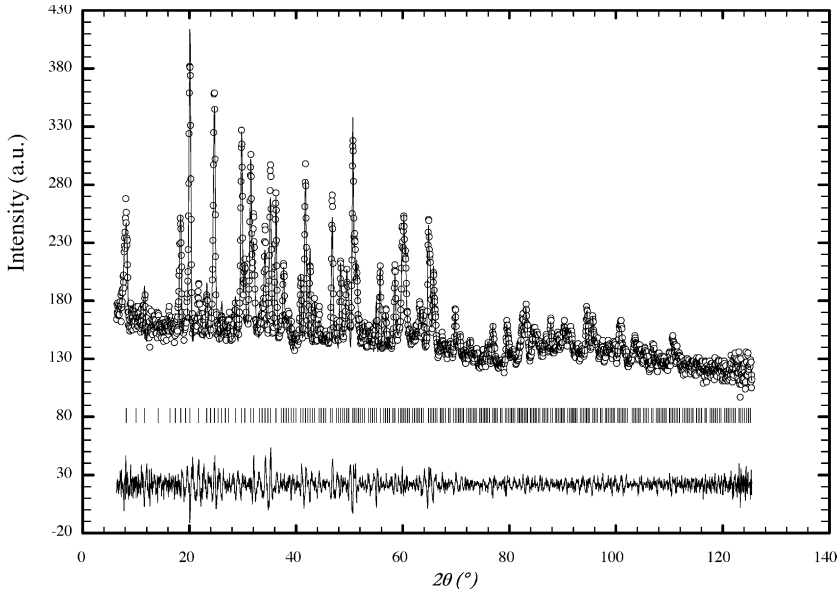

Fig. 1. Comparison of observed (crosses) and calculated (solid line) intensities for WPA-6 at 298 K. The difference pattern appears below. The vertical bars, at the bottom, indicate position of the reflections.

The dioxonium ion $H_5O_2^+$, which is part of the structure of dodecatungstophosphoric acid hexahydrate $H_3PW_{12}O_{40}6H_2O$ (WPA-6), is the subject of extensive theoretical and experimental investigations devoted to study the nature of the high proton mobility in water [13–15]. The crystal structure of this ion is precisely defined only in a few studies [16–22]. To our best knowledge, no attempt has been done to investigate temperature-induced changes of $H_5O_2^+$ crystal structure, although it is well known that biochemical and catalytic activities of these compounds are temperature-dependent [9]. The crystal structure of the WPA-6 is a bcc packing of $PW_{12}O^3_{40}$ and $H_5O_2^+$. Brown et al. [17] have found that Keggin's anions in WPA-6 are stabilized by $H_5O_2^+$ ions, whereas Miocˇ et al. [23,24] discussed the temperature-dependent dynamic equilibrium between different proton species ($H_9O_4^+$, $H_7O_3^+$, $H_5O_2^+$, H_3O^+, H^+). Recently, we have shown that, in WPA-6 at about 320 K, a nonconvergent reversible phase transition exists and is associated with the reversible temperature-dependent partial reduction/oxidation of some W^{6+} and W^{5+} ions provoked by the presence of different proton species in this compound [25]. With the temperature increase, the $H_5O_2^+$ ions could reorganize and different forms of hydrated protons H_3O^+, $H_7O_3^+$,... OH or H^+ could be formed. As proton species are responsible for conductive, catalytic and many other properties of heteropolyacids, we have decided to investigate the structure of $H_5O_2^+$ ions, the temperature-induced dynamic equilibrium of proton species and changes of WPA-6 crystal structure and microstructure with the neutron powder diffraction (NPD) method.

2. Experimental

The polycrystalline material of WPA-6 was prepared from the commercial Phosphotungstic Acid for Microscopy $H_3(P(W_3O_{10}))_{aq}$ (Fluka, CH-9470 Buchs, #79690). To obtain the WPA-6, the starting material was treated at 353 K for 1 h. The isotopic exchange H_2 X D_2 was done in a dry box (humidity <20%). The WPA-6, dissolved in D_2O, was treated at 323 K until water evaporation. Re-crystallization was performed for 11 times. Deuterated polycrystalline material was transported in a glass vial.

The IR spectra of deuterated samples were recorded, on a 983 G Perkin-Elmer spectrophotometer, as a suspension in Nujol oil on KBr windows.

For NPD experiments, the deuterated polycrystalline material was carefully placed in a vanadium container. The samples in the vanadium container were kept isolated from humidity during the data recording. A CAF rhodorsil siliceous seal was used to prevent isotopic exchange D_2 X H_2. The NPD data for Rietveld structure refinement were collected on a 3T2 High-resolution Neutron Powder diffractometer, equipped with a cryofurnace, at the ORPHEE nuclear reactor at Laboratoire Le´on Brillouin (CEA–CNRSSaclay, France). The powder patterns were recorded at 10, 83, 298, 318, 338 and 358 K with temperature stability better than 0.5 K. Unfortunately, only the data collected at 298 and 338 K were taken from the deuterated sample, due to the fast H_2 !D_2 exchange at atmospheric conditions. The wavelength of the incident neutron beam was set to 1.2252 $\mathring{A}$. A Ge (335) monochromator was used. The collimating angles were a_1 =a_2 =10V. The NPD data were collected (24 h per record) in 2h regions 5–125.5j with constant steps: 0.05j 2h.

3. Results

The starting structural model taken from Brown et al. [17], neutron single crystal structure data at 298 K of WPA-6, was refined on the NPD data with the aid of the FullProf computer program [26]. The TCH-pV modified pseudo-Voigt profile function was applied. The peak base width was set to the six values of reflections half-width. The instrumental resolution function (U = 0.278, V = 0.345, W = 0.150) was included in the refinement, allowing instrumental and specimen contributions to the diffraction profiles to be deconvoluted. The Warren–Averbach line-broadening method has been applied [27] using the Breadth computer program [28]. Microstructure parameters (crystallite sizes and strains) have been calculated in three directions [100], [110] and [111]. The background is refined with the Fourier filtering method [26]. Window for Fourier filtering was set to 750.

The final Rietveld plot of the data recorded at 298 K is presented in Fig. 1. Rietveld plots at other temperatures are similar. Reliability factors and statistical parameters are presented in Table 1. Refined values of the unit-cell parameters, Debye characteristic temperatures, fractional coordinates and isotropic temperature vibration

parameters are presented in Table 2. Fractional coordinates and isotropic temperature vibration parameters for all atoms are refined, constrained only by the symmetry restrictions of the space group. Site occupation factors for D_w/H_w and D_a/H_a for the data collected at 298 and 338 K are constant within estimated standard deviations, indicating the presence of 70% of deuterium and 30% of hydrogen, which is in agreement with the IR results.

Table 1
Reliability and statistic parameters of the Rietveld refinement for the WPA-6 at different temperatures [26]:

$$R_{wp} = 100 \left[\frac{\sum_i w_i (y_{oi} - y_{ci})^2}{\sum_i w_i y_{oi}^2} \right]^{1/2}; \quad R_p = 100 \frac{\sum_i |y_{oi} - y_{ci}|}{\sum_i y_{oi}};$$

$$R_{exp} = 100 \left[\frac{N - P}{\sum_i w_i y_{oi}^2} \right]^{1/2}; \quad v = \frac{R_{wp}}{R_{exp}};$$

$$R_{Bragg} = 100 \frac{\sum_k |I_k - I_{ck}|}{\sum_k I_k}$$

T [K]	10	83	298	318	338	358
R_{wp}	2.67	2.47	3.66	2.54	3.27	2.67
R_p	2.17	2.03	3.03	2.14	2.72	2.23
R_{exp}	1.76	1.76	2.22	1.78	2.27	1.79
v^2	2.30	1.97	2.72	2.04	2.07	2.23
R_{Bragg}	2.31	3.46	3.20	3.45	2.44	3.18

Table 2
Unit-cell parameters, Debye temperature, fractional coordinates, thermal vibration parameters, site occupation factors (SOF) for O_w and H_w and percentage of deuterisation (% deuterium) for D_w/H_w and D_a/H_a for the WPA-6 at different temperatures

Atom	T [K]	10	83	298	318	338	358
	a [Å]	12.0772(2)	12.0928(2)	12.1507(2)	12.1556(2)	12.1607(3)	12.1662(1)
	H [K]	206(11)	209(13)	202(9)	209(10)	215(10)	222(11)
W	x	0.7589(5)	0.7592(5)	0.7591(5)	0.7602(5)	0.7575(5)	0.7584(4)
	y=z	0.9575(3)	0.9576(3)	0.9575(3)	0.9570(4)	0.9564(3)	0.9565(3)
	U_{iso} [Å^2]	0.0035(3)	0.0058(4)	0.021(1)	0.020(1)	0.019(1)	0.019(1)
P	x=y=z	0.75	0.75	0.75	0.75	0.75	0.75
	U_{iso} [Å^2]	0.0015(7)	0.003(1)	0.014(3)	0.014(4)	0.021(4)	0.022(5)
O_a	x=y=z	0.8236(4)	0.8249(4)	0.8255(4)	0.8225(4)	0.8167(3)	0.8174(3)
	U_{iso} [Å^2]	0.0032(2)	0.0055(4)	0.017(1)	0.017(2)	0.016(2)	0.016(2)

O_b	x=y	0.6552(2)	0.6555(3)	0.6553(2)	0.6555(3)	0.6556(2)	0.6594(2)
	z	0.5065(4)	0.5064(4)	0.5072(3)	0.5077(4)	0.5073(4)	0.5100(3)
	U_{iso} [A° 2]	0.0031(2)	0.0050(4)	0.0201(8)	0.020(1)	0.0160(8)	0.016(1)
O_c	x=y	0.8719(3)	0.8723(3)	0.8722(3)	0.8716(3)	0.8733(4)	0.8714(3)
	z	0.0296(4)	0.0257(4)	0.0237(4)	0.0252(5)	0.0218(4)	0.0222(4)
	U_{iso} [A° 2]	0.0035(2)	0.0051(4)	0.0231(9)	0.023(1)	0.022(1)	0.022(1)
O_d	x	0.7321(3)	0.7325(3)	0.7332(4)	0.7317(5)	0.7332(5)	0.7339(4)
	y=z	0.0556(2)	0.0554(2)	0.0554(3)	0.0540(3)	0.0531(3)	0.0523(2)
	U_{iso} [A° 2]	0.0032(2)	0.0049(4)	0.030(1)	0.030(1)	0.029(1)	0.029(1)
O_w	x	0.75	0.75	0.75	0.75	0.75	0.75
	y	0.1548(7)	0.1562(7)	0.1517(8)	0.149(1)	0.1499(8)	0.1555(8)
	z	0.25	0.25	0.25	0.25	0.25	0.25
	U_{iso} [A° 2]	0.0052(6)	0.0095(8)	0.049(3)	0.048(4)	0.048(3)	0.048(4)
	SOF	0.5	0.5	0.5	0.5	0.5	0.5
D_w/H_w	x	0.738(1)	0.742(2)	0.743(1)	0.749(1)	0.746(1)	0.745(2)
	y	0.1124(8)	0.113(1)	0.1075(9)	0.1148(8)	0.107(1)	0.109(2)
	z	0.1845(8)	0.185(1)	0.1882(9)	0.1813(9)	0.1841(9)	0.186(2)
	U_{iso} [A° 2]	0.0092(7)	0.016(1)	0.038(3)	0.032(3)	0.039(3)	0.039(3)
	SOF	0.5	0.5	0.5	0.5	0.5	0.5
	% deuterium	0	0	70	0	70	0
D_a/H_a	x	0.75	0.75	0.75	0.75	0.75	0.75
	y=z	0.25	0.25	0.25	0.25	0.25	0.25
	U_{iso} [A° 2]	0.0062(8)	0.0105(9)	0.041(2)	0.044(4)	0.045(2)	0.043(5)
	% deuterium	0	0	70	0	70	0

In parentheses are estimated standard deviations (ESD).

Inspite of the loss of deuterium atoms at the other temperatures, the high resolution of the diffractometer allowed us to locate precisely all hydrogen atoms (Table 2). Selected inter-atomic distances and angles at different temperatures are compared in Table 3.

4. Discussion

4.1. General description of the WPA-6 crystal structure

The crystal structure of WPA-6 consists of Keggin's anions $PW_{12}O_{40}^{3}$ and dioxonium ions $H_5O^{+}_2$. In the Keggin's anion, PO_4 central tetrahedron is surrounded by 12 WO_6 octahedra. In these octahedrons, there are four groups of three edge-shared octahedra (triplets) having a common oxygen vertex connected to the central phosphorous atom. Therefore, four classes of symmetry equivalent oxygens could be recognized: PUO_aUW, WUO_bUW connecting two triplets by corner sharing, WUO_cUW connecting two triplets by edge sharing and $WUO_dUH_wUO_w$, where O_d are bridging atoms to dioxonium ions (Fig. 2). The dioxonium ions are almost planar. The two interpenetrating substructures, with subsequent indexes 1 and 2 in subscript, are statistically distributed with one half population each (Fig. 3). Additionally, according to

Table 3
Selected inter-atomic distances and angles for the WPA-6 at different temperatures

Inter-atomic distances and angles	T [K]					
	10	83	298	318	338	358
Distances within Keggin's anion [A°]						
WUO_a	2.417(6)	2.404(6)	2.408(6)	2.433(7)	2.508(5)	2.499(5)
WUO_b	1.900(5)	1.906(6)	1.911(6)	1.917(7)	1.893(6)	1.899(5)
WUO_c	1.921(6)	1.901(6)	1.900(6)	1.897(7)	1.907(6)	1.898(6)
WUO_d	1.706(5)	1.705(4)	1.711(5)	1.702(6)	1.689(5)	1.674(5)
PUO_a	1.539(5)	1.569(5)	1.588(4)	1.526(5)	1.404(4)	1.421(4)
PUO_d	5.223(3)	5.228(3)	5.251(3)	5.230(5)	5.216(5)	5.204(4)
$O_a...O_{ai}$	2.512(6)	2.562(7)	2.593(6)	2.492(7)	2.293(5)	2.320(5)
$O_a...O_b$	2.900(6)	2.901(6)	2.909(6)	2.907(7)	2.921(5)	2.862(5)
$O_a...O_c$	2.621(6)	2.560(7)	2.539(7)	2.605(8)	2.678(6)	2.658(6)
$O_b–O_{bii}$	2.540(5)	2.550(5)	2.544(5)	2.540(6)	2.550(5)	2.570(5)
$O_b...O_c$	2.672(4)	2.671(5)	2.683(5)	2.677(5)	2.695(5)	2.635(4)
$O_b...O_d$	2.811(5)	2.817(5)	2.833(6)	2.811(7)	2.805(6)	2.833(6)
$O_c...O_{ciii}$	2.693(5)	2.624(6)	2.603(6)	2.641(7)	2.553(6)	2.595(6)
$O_c...O_d$	2.806(5)	2.809(5)	2.820(6)	2.816(6)	2.797(6)	2.788(5)
Distances within $H_5O^+_2$ [A°]						
$O_w–H_w$	0.95(1)	0.95(2)	0.93(1)	0.93(1)	0.96(1)	0.97(2)
$O_w...H_a$	1.115(9)	1.135(9)	1.19(1)	1.23(1)	1.22(1)	1.15(1)
$O_w...O_w$	2.23(2)	2.27(2)	2.38(2)	2.46(2)	2.44(2)	2.30(2)
Distances between anion and $H_5O^+_2$ [A°]						
$O_d...H_w$	1.70(1)	1.72(2)	1.74(1)	1.73(1)	1.73(1)	1.77(2)
$O_d...O_w$	2.646(8)	2.658(8) [j]	2.65(1)	2.66(1)	2.68(1)	2.721(9)
Angles within $H_5O^+_2$ and between anion and $H_5O^+_2$						
$H_w–O_w–H_w$	115(2)	112(3)	109(2)	127(2)	114(2)	109(3)
$H_w–O_w...H_a$	123(1)	124(2)	125(1)	116(1)	123(1)	126(3)
$O_w–H_w...O_d$	169.2(9)	169(1)	166(1)	173(1)	169(1)	167(2)
$O_d...O_w...O_d$	126.1(2)	125.5(2)	127.5(2)	128.5(3)	127.8(2)	125.0(2)

The symmetry transformations are: (i) x, 1.5y, 1.5z; (ii) 1.5y, z, 1.5x; (iii) y, z, x; (iv) 1.5z, 1.5x, y; (v) z, x, y. In parentheses are ESDs.

the following equilibrium $H_5O_2^+ \chi H_3O^+ + H_2O \; X \; H^+ + 2H_2O$, various forms of hydrated proton entities take part in the structure at the same time. This was confirmed by the IR, Raman and IINS studies on WPA-6 [23,24,29]. Furthermore, the equilibrium may influence the oxidation level of heteroatoms; that implies partial reduction of some W^{6+} into W^{5+}, which was confirmed by the X-ray powder diffraction (XRPD) and Raman studies on WPA-6 [25]. Therefore, this structure is not completely described by Brown et al. [17], due to the fact that they did not

take in consideration the existence of a temperaturedependent dynamic equilibrium of different hydrated proton species and partial reduction of some W^{6+} into W_{5+}.

Fractional coordinates and isotropic vibration temperature parameters are refined without constraints in this work. Only space group symmetry constraints are applied. Constraints on the temperature vibration parameters for oxygen atoms within Keggin's anion and phosphorous atoms have been applied to the XRPD data [25]. The explanation for such behavior is the following: neutrons scatter from the cores of the atoms and therefore a nonperiodic change in the electronic structure of atoms does not effect as a disorder for neutron diffraction. In contrary to the neutrons, the X-rays diffract from the electron shells and therefore are sensitive to a nonperiodic change in the electronic structure of a material. Due to the partial reduction of some W^{6+} into W^{5+} [25], the electronic structure of WPA-6 changes nonperiodically and therefore constraints in the refinement applied to the

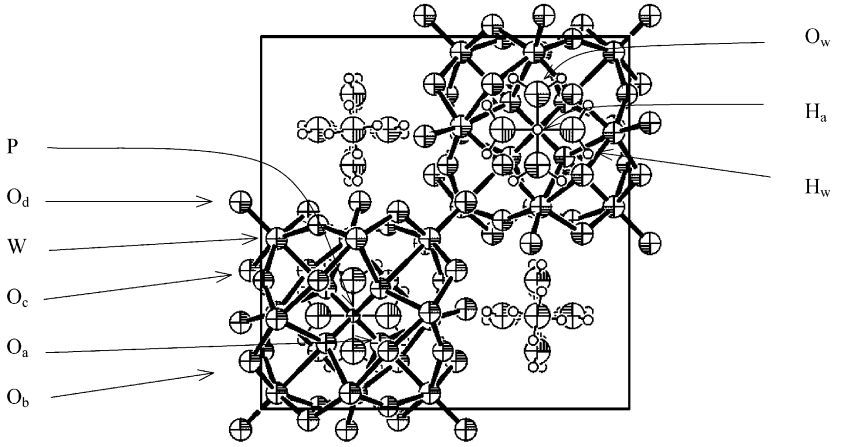

Fig. 2. Structure of WPA-6 at 10 K (Ortep [46] representation).

XRPD data have been presented.

Our previous XRPD and Raman results [25] indicate the existence of significant structural changes at about 320 K. The reliability factors and statistical parameters of the refined structure and profile parameters (Table 1), indicate that the crystal structure

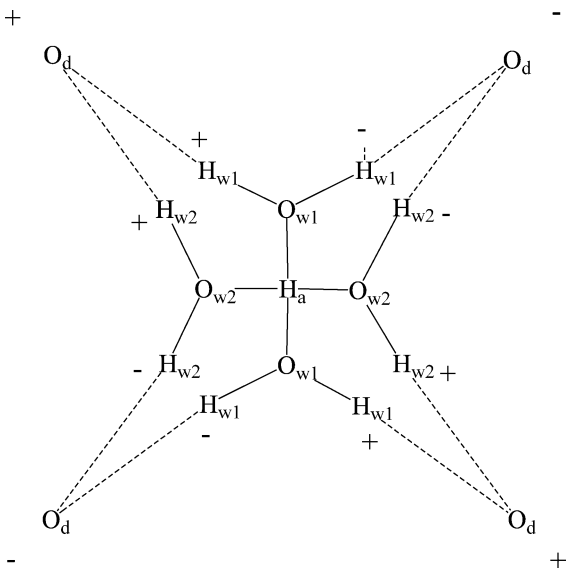

Fig. 3. Schematic representation of disorder in the dioxonium ion structure and its connection to the Keggin's polyanions. Symbol + (respectively,) indicate that the atoms are above (respectively, below) the plane of the figure.

model fit the experimental data at all investigated temperatures. The WPA-6 nuclear density map (F_{obs}) for NPD data collected at 298 K (Fig. 4), indicate that positions for hydrogen atoms in $H_5O_2^+$ are welldefined. From the regression analysis, we have found that unit-cell parameters change linearly with temperature. From the slope of the graph a=f(T), where a is the unit-cell parameter and T is the temperature, we have found a linear coefficient of thermal expansion a=(2.56 F0.01) 10 ^{4} A$^{\circ}$ K ^{1}. The calculated value of Debye temperature (Table 2), is constant within estimated standard deviations (ESDs) in the investigated temperature region, which is in agreement with the value calculated from the data obtained from neutron diffraction for a single crystal [17]. These results indicate that the $Pn\bar{3}m$ space group preserves between 10 and 358 K.

4.2. The dioxonium ion

To our best knowledge, a small number of neutron diffraction studies have been performed on compounds containing a dioxonium ion [16–22]. Excluding the structure of WPA-6, the dioxonium ion presents the following characteristics (Table 4). An $O_w...O_w$ distance is in the range (2.40–2.46 Å) with a proton situated on the $O_w...O_w$ axis and $O_wUH_a...O_w$ angle in the range (172–180j). The proton is generally located on a special symmetry position of the space group leading to identical O_wUH_a inter-atomic distances, or gives similar O_wUH_a values. The dioxonium

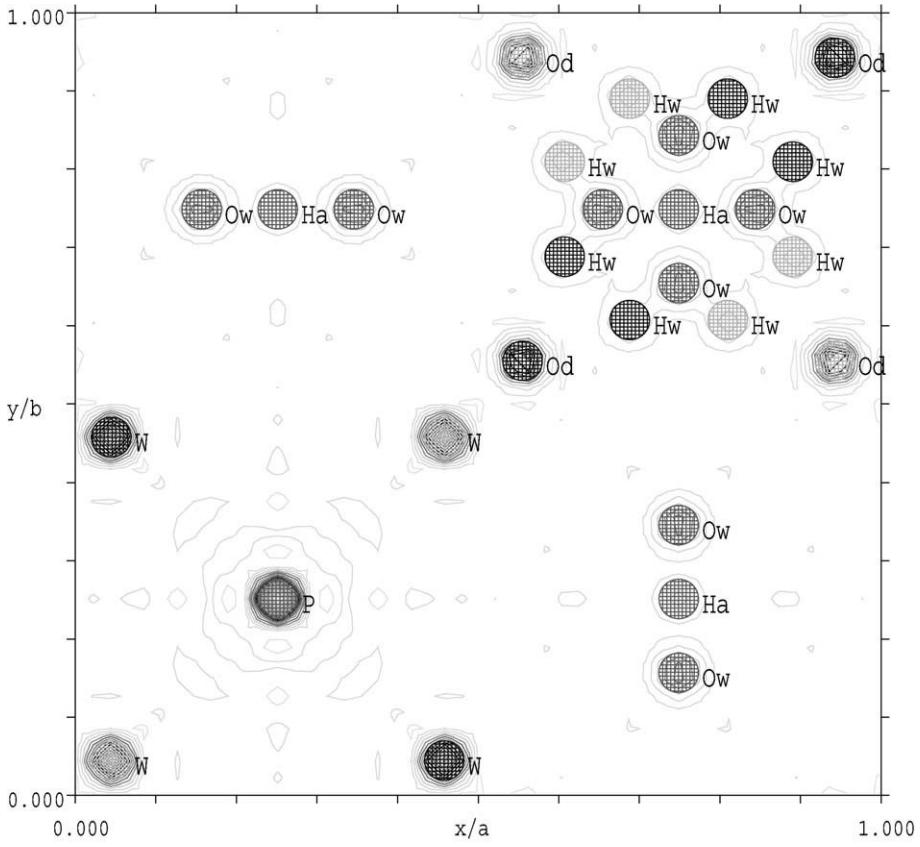

Fig. 4. Nuclear density map (F_{obs}) for NPD data collected at 298 K. Projection is in xy-plane for z=0.25. Conture levels at 0.26 fm Å^{-3}.

ion, which can be described by the following system $(H_3OUOH_2)^+$, could exhibit different symmetries for the oxonium ion: trigonal pyramidal (symmetry C_S, Fig. 5b and d) and flat equilateral triangular (symmetry C_2, Fig. 5a and c) structures. Ab initio calculations [13–15] have shown that the two conformations (Fig. 5a and b) have similar

energies when they are staggered. The situation when two hydrogen atoms (Fig. 5d) or four hydrogen atoms (Fig. 5c) are in eclipsed position is evidently less stable. Excluding WPA-6, all the structures give a dioxonium ion in the staggered conformation with the trigonal pyramidal oxonium ion (Fig. 5b). A rapid survey of the structure of the dioxonium ion obtained from X-ray single crystal diffraction at low temperature [30–33] or near room temperature [34–37], where the hydrogen atoms are located give similar results. Therefore, for the $H_5O_2^+$ detection in a crystal structure, an $O_w...O_w$ distance in the range (2.40–2.46 Å) could be used as the most frequent.

The structure of the dioxonium ion at 10 K in WPA-6 can be described by the following system $(H_2OUHUOH_2)^+$ (Fig. 6). The two water molecules present usual inter-atomic H_wUO_w distances [38] (hd=0.95(1) A˚ i averaged for all the temperatures).

The $H_wUO_wUH_w$ valence angle is 115(2)j exhibiting a slightly higher value than the averaged value suggested by Chiari et al. [38] ($hH_wUO_wUH_w$ =107.2ji over 142 neutron values belonging to inorganic compounds). A recent work [39] based on 49 well-refined organic and organometallic neutron diffraction crystal structures has established a relation between the

Table 4
Neutron diffraction results on $H_5O^+_2$ cation structure

Reference	[17]	[18]	[19]	[20]	[21]				
T [K]	298	298	20	233	298	298	298	118	333
Compound no.	I	II	III	IV	Va	Vb	Vc	Vc	Vc
$O_w...O_w$ [Å]	2.370(5)	2.436(2)	2.434(5)	2.40(1)	2.440(3)	2.453(4)	2.440(4)	2.425(3)	2.460(5)
O_wUH_w [Å]	0.951(3)	0.996(4)	0.975(8)	0.99(1)	0.983(3)	0.979(2)	0.964(7)	0.978(4)	0.967(9)
			0.984(9)	0.99(1)	0.992(3)	0.982(2)	0.972(7)	0.976(5)	0.970(9)
				0.97(1)					
				0.96(1)					
$O_w...H_a$ [Å]	1.185(5)	1.128(4)	1.215(4)	1.22(1)	1.221(1)	1.227(2)	1.221	1.216	1.228
		1.310(4)		1.18(1)					
$H_wUO_wUH_w$ [j]	118.7(5)	110.4(3)	107(1)	109(2)	110.7(2)	110.9(2)	110.8(6)	110.5(4)	111.7(8)
		107.2(3)		109(2)					
$H_wUO_wUH_a$ [j]	120.7(2)	112.6(3)	114(1)	124(2)	112.8(2)	112.3(2)	112.3	112.9	111.0

		108.1(3)	108(1)	114(1)	117.6(2)	117.4(2)	117.2	115.3	119.7
		115.4(3)		126(1)					
		111.9(3)		109(2)					
Conformation	5c	5b	5b	5d	5d	5d	5d	5d	5d

Compounds are: I ($PW_{12}O_{40}$)3(H_5O_2); II (H_5O_2)[$C_6H_2(NO_2)_3SO_3$]2H_2O; III U(H_2O)$_6$(H_5O_2)(CF_3SO_3)$_4$; IV (H_5O_2)Br; V (a) Y$H(C_2O_4)3H_2O$, (b) Y$D(C_2O_4)3D_2O$, (c) Y$X(C_2O_4)3X_2O$ (X=H/Di50%). Conformations refer to the schematic representation defined in Fig. 5.

O...O_w...O angle and the $H_wUO_wUH_w$. For an O...O_w...O angle in the range (120–130j), as observed in WPA-6, the mean value for $H_wUO_wUH_w$ is 109.5(6)j. Therefore, the value obtained at 10 K is consistent with the hydrogen-bonding network chaining the dioxonium ion to the Keggin's ion. The external hydrogen bond H_w...O_d between dioxonium ion and Keggin's anion is about 1.7 A˚ and could be classified as a moderate hydrogen bond [16]. These characteristics are typical of the dioxonium ion (Table 4). Nevertheless, three specific behaviors of the $H_5O_2^+$ structure at 10 K exist: (i) the link between the two water molecules is formed by two extremely short bonds between the proton and the water molecules, leading to one of the strongest hydrogen bonds [16], and to an O_w...O_w distance smaller by 0.17 A˚ from the usual value (f2.4 A˚ , Table 4); (ii) the $H_wUO_wUH_a$ angle (123(1)j) is one of the highest values observed (hH_wUO_w...H_ai= 115j averaged over 20 values); (iii) the dioxonium ion contains a flat equilateral oxonium moiety ($H_wUO_wUH_aUO_wU$ H_w torsion angle =20(3)j) leading to the noncomplete eclipsed conformation (Figs. 5c and 6b). The explanation for such a particular behavior lies in the connection between the dioxonium ion and the Keggin's anion.

The structure of the dioxonium ion at the highest recorded temperature (358 K) remains similar to the structure observed at 10 K. However, significant changes could be observed at 318 K, which corresponds to the T_c of the

nonconvergent phase transition observed previously [25] (Fig. 7). At 318 K, the dioxonium ion takes a completely flat conformation

($H_wUO_wUH_aUO_wUH_w$ torsion angle =3(3)j), with a long $O_w...O_w$ distance (reaching the usual dioxonium value, Table 4) and a large $H_wUO_wUH_w$ value. Local symmetry of $H_5O_2^+$ changes reversibly with temperature changes D_2 (10 K) X D_{2h} (318 K) X D_2 (358 K). Connections with the Keggin's ion do not change, i.e. ($dO_d...H_w$) remains close to 1.73(1) Å at all temperatures. The consequence of the structure changes of the dioxonium ion at 318 K is an extension of the possibility of changing the dynamic equilibrium between proton species.

4.3. Disorder in the structure of WPA-6

In the previous sections, we have already noticed different types of disorder which take place in the WPA-6 structure in the range (10–358 K): (i) static disorder of water molecules, (ii) hydrogen bonds disorder inside the dioxonium ion (configurational disorder), (iii) substitutional disorder of the tungsten ion (partial reduction from W^{6+} to W^{5+}). Here, we will investigate more precisely their nature.

First, static disorder exists in the dioxonium ion due to the localization of two disordered interpenetrating substructures of $H_5O_2^+$ form statistically one half populated tetramer (dimer of water molecules and proton, Figs. 3 and 4).

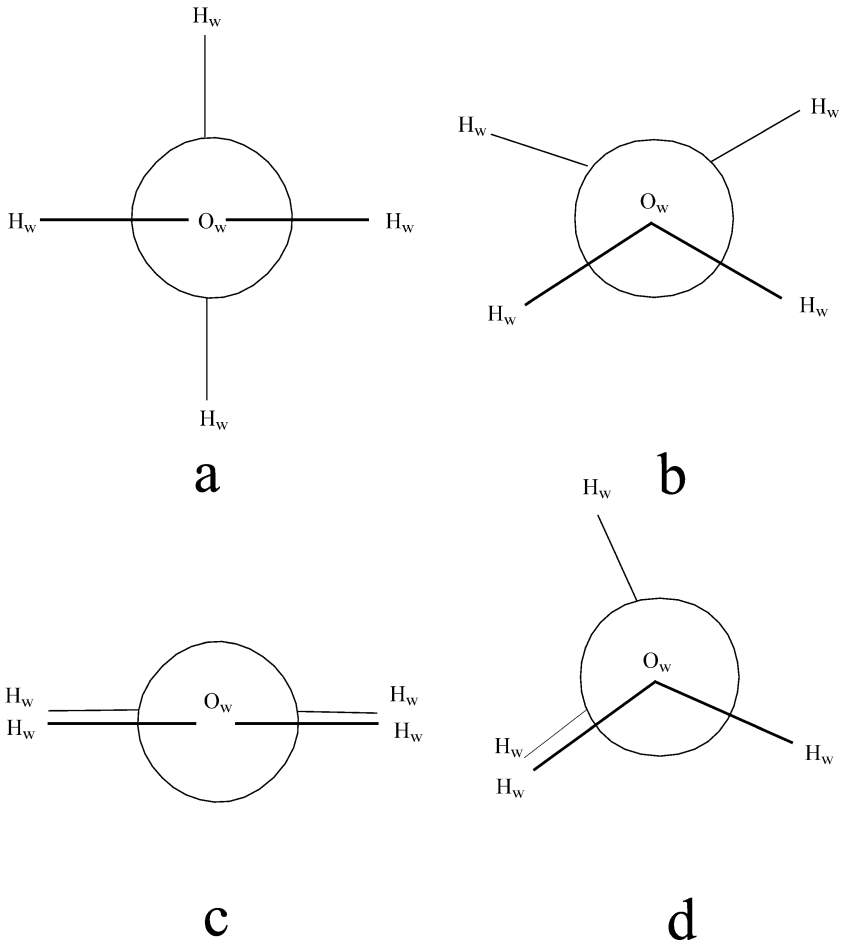

Fig. 5. Schematic representation of different $H_5O^+_2$ conformations: (a) H_3O^+ in a flat equilateral triangular structure (symmetry C_2)—staggered conformation of H_w atoms, (b) H_3O^+ in a trigonal pyramidal structure (symmetry C_S)—staggered conformation of H_w atoms, (c) H_3O^+ in a flat equilateral triangular structure (symmetry C_2)—four H_w atoms are in eclipsed position, (d) H_3O^+ in a trigonal pyramidal structure (symmetry C_S)—two H_w atoms are in eclipsed position.

Second, a disorder in hydrogen bonds in the $H_5O_2^+$ ion occurs. Internal hydrogen bonds H_aUO_w in $H_5O_2^+$ are very strong hydrogen bonds ($dH_aUO_w = 1.115(9)$ Å) indicating the presence of a switching mechanism, which can be described as a configurational disorder leading to a proton transfer:

O_w...H_aUO_w X O_wUH_a...O_w. This mechanism is coherent with the fact that for strong $^+$OUH...O or O...HUO bonds, the potential energy surface is almost flat, i.e. potential barriers are low [16] and is analogous to the proton transfer observed in polyglucine and N-methyl acetamide [40]. The structure of the dioxonium ion is symmetric (H_a lies in a special position of the space group). The isotropic vibrational parameters of the atoms in WPA-6 exhibit an interesting behavior. At low temperatures (10 K), all the oxygen atoms of the Keggin's ion adopt a very close value while O_w present a ratio

$U_{iso}(O_w)/U_{iso}(O_{Keggin})$=1.6. At this temperature in the dioxonium ion, we have the following order $U_{iso}(O_w)<U_{iso}(H_a)<U_{iso}(H_w)$. Between 298 and 358 K, the reverse trend is observed $U_{iso}(O_w)>U_{iso}(H_a)>U_{iso}(H_w)$. These behaviors lead to the following conclusion: the proton transfer (involving H_a

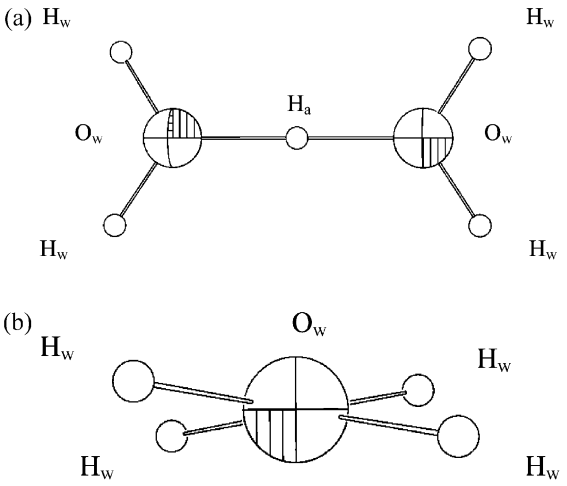

Fig. 6. Dioxonim ion structure of WPA-6 at 10 K (a) all H_w are at the equal distance to the H_a, (b) plane perpendicular to the O_w–H_a– O_w axis.

atom) which begins around room temperature, continues after T_c, while the structure change of the two water molecules (proved in the previous section, Fig. 7) is reversible.

Third, a substitutional disorder concerns the partial reduction of some tungsten ions (W^{6+}!W^{5+}).

4.4. Temperature-induced change of microstructure in WPA-6

The microstrain in the center of the average volume-weighted crystallite is negligible at all temperatures, indicating that Schottky and Frenkel defects are not dominantly present in WPA-6. Crystallites are isometric at all temperatures. At 10 K, crystallites are average 240(10) Å in diameter. At 83 K, the average diameter of crystallites are the same within the estimated standard error. At 298 K, the average crystallite size diameter decreases to 190(5) Å and does not change within estimated errors at 318 and 338 K. At 358 K, the average crystallite size diameter decreases further to 170(5) Å. The decrease of the average volume-weighted crystallite diameter with temperature increase indicates an increase of Bjerum [41], Nagle [42], Dunitz [43] and other defects. A nonsystematic change of the crystallite size at about 320 K was associated with the phase transition.

Microstructure parameters differ significantly for

XRPD [25] and NPD data. The diameter of the average crystallite obtained from NPD data is two to three times smaller than from XRPD data. H, P, Wand O atoms contribute more equally to the neutron scattering power than to the X-ray scattering power of the crystal. Therefore, crystallites measured from the NPD line-broadening analysis should be smaller or at least equal to the crystallites measured from the XRPD line-broadening analysis.

4.5. Phase transition in WPA-6 at about 320 K

Two reversible temperature-dependent processes have been noticed in WPA-6:

Partial reduction/oxidation of tungsten ion $W^{6+} \rightleftharpoons W^{5+}$ and

Dynamic equilibrium of proton species $H_5O_2^+ \rightleftharpoons H_3O^+ + H_2O \rightleftharpoons H^+ + 2H_2O$.

From the XRPD and Raman investigations [25], we have found that reversible nonconvergent phase transition exist in WPA-6 at about 320 K. The XRPD result shows that: (i) Keggin's ion, particularly PO_4 tetrahedra change

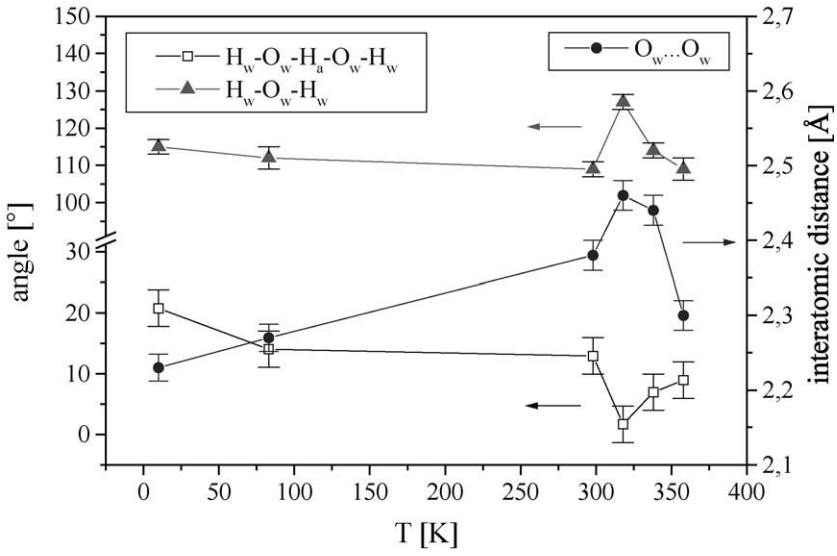

Fig. 7. Some geometrical parameters (inter-atomic distance O_w...O_w, inter-atomic angle $H_wUO_wUH_w$ and torsion angle $H_wUO_wUH_aUO_wUH_a$) behavior of $H_5O^+_2$ in the range 10–358 K. Peaks at around 320 K are characteristic of the phase transition.

(shrink by approximately 10%) near T_c and (ii) the crystal structure space group preserves during the phase transition; therefore the phase transition near 320 K is nonconvergent. From Raman investigations, we have found that: (i) the local symmetry of PO_4 changes expressively with temperature changes near T_c and (ii) charge transfer exists in WPA-6 near T_c !(broadening of r_1 (PUO_a) valence vibrational band). Changes in the structure geometry of Keggin's anion, microstructure, color and existence of charge transfer in WPA-6 at about 320 K indicate the presence of partial reduction/oxidation W^{6+} X W^{5+} near T_c. Partial reduction/ oxidation W^{6+} X W^{5+} occurs very easily due to the fact that tungsten is a mixed valence ion. The results of IINS and IR spectroscopy indicate that a temperature-dependent dynamic equilibrium $H_5O_2^+$ X $H_3O^+ + H_2O$ X $H^+ + 2H_2O$ exists in WPA-6 [23]. Recently, Essayem et al. [44] have shown by H^2 MAS NMR and IINS spectroscopies that various protonic species are present in deuterated WPA-n and that their relative amount is a function of temperature, supporting the results of Mioc˘ et al. [23,24,29].

One can estimate that the number of W^{5+} in WPA-6 is small. The dynamic equilibrium $H_5O_2^+$ X $H_3O^+ + H_2O$ X $H^+ + 2H_2O$ is slightly shifted to the right-hand side and therefore a small number of $H_5O_2^+$ are reorganized. Consequently, if only one of the 12 W^{6+} in the Keggin's polyion $[PW_{12}O_{40}]^3$ is reduced to W^{5+}, it is sufficient to change the total valence of the polyion from 3 to 4. Due to the fact that the dynamic equilibrium of the proton species is slightly shifted to the right-hand-side, the number of W^{5+} when comparing to W^{6+} in the WPA-6 is a less then 1/12. Therefore, the formal charge of the Keggin's polyion remains the same while the effective charge changes. Moreover, Marosi et al. [45] pointed out that Keggin's polyions in dehydrated samples are alternatively + and charged, suggesting that the overall charges of the same type of polyions in one specimen varies remarkably—even in sign. In our opinion, at about 320 K, the change in charges of Keggin's polyanion in WPA-6 is significantly smaller, but it exists. The position in the structure, where tungsten ions are reduced, should be treated as defects and should reflect on the crystallite microstructure. NPD results clearly indicate that average crystallites change in diameter by about 20% near the T_c.

5. Conclusion

There are two interconnected temperature-dependent reversible processes in WPA-6 that reflect on the crystal structure and microstructure: (i) change of the dynamic equilibrium of hydrate species and different proton species and (ii) partial reduction/oxidation of some tungsten ions. Expressive changes are an abrupt decrease of the PUO_a bond length and increase of the planarity of $H_5O_2^+$ near 320 K. The average volumeweighted crystallite size changes nonsystematically near 320 K suggesting an increase of the defects in WPA-6. With temperature increase, the number of reorganized $H_5O_2^+$ and reduced W^{6+} increase, resulting in a nonconvergent reversible phase transition at about 320 K. The phase transition is associated with changes in: $H_5O_2^+$ and PO_4 local symmetry, structure geometry, number of decomposed $H_5O_2^+$ and reduced W^{6+} and quantity of defects and disorder in the crystal structure.

References

[1] M.T. Pope, Heteropoly and Isopoly Oxometalates, Springer, Berlin, 1983.

[2] M.T. Pope, A. Mu¨ller, Polyoxometalates: From Platonic Solids to Anti-Retroviral Activity, Kluwer Academic Publishing, London, 1994.

[3] M. Raynaud, J.C. Chermann, F. Plata, C. Jasmin, G. Mathe´, C. R. Acad. Sci. Ser., D 272 (1971) 347.

[4] J.C. Chermann, F. Sinoussi, C. Jasmin, Biochem. Biophys. Res. Commun. 65 (1975) 1229.

[5] G.-S. Kim, H. Zeng, J.T. Rhule, I.A. Weinstock, C.L. Hill, Chem. Commun. (1999) 1651.

[6] M.K. Harrup, G.-S. Kim, H. Zeng, R.P. Johnson, D. VanDerveer, C.L. Hill, Inorg. Chem. 37 (1998) 5550.

[7] G.-S. Kim, H. Zeng, D. VanDerveer, C.L. Hill, Angew. Chem., Int. Ed. 38 (1999) 3205.

[8] M.M. Marisic, J. Am. Chem. Soc. 62 (1940) 2312.

[9] T. Okuhara, N. Mizuno, M. Misono, Adv. Catal. 41 (1996) 113.

[10] O. Nakamura, T. Ogino, T. Kodoma, Solid State Ion. 3 (4) (1981) 347.

[11] Ph. Colomban (Ed.), Protonic Conductors, Solid Membranes andGels,CambridgeUniv.Press,Cambridge, 1992,pp.38–56. [12] B. Tell, S. Wagner, Appl. Phys. Lett. 33 (1978) 837.

[13] M. Chaplin, Water Structure and Properties, http://www.sbu. ac.uk/water/index.html, 2001.

[14] D. Marx, M.E. Tuckerman, J. Hutter, M. Parrinello, Nature 397 (1999) 601.

[15] F.F. Muguet, J. Mol. Struct. (Teochem) 368 (1996) 173.

[16] G.A. Jeffrey, An Introduction to Hydrogen Bonding, Oxford Univ. Press, New York, 1997, Chaps. 3.5 and 3.6.

[17] G. Brown, M. Noe-Spirlet, W. Busing, H. Levy, Acta Crystallogr., B 33 (1977) 1038.

[18] J.O. Lundgren, R. Tellgren, Acta Crystallogr., B 30 (1974) 1937.

[19] F.A. Cotton, C.K. Fair, G.E. Lewis, G.N. Mott, F.K. Ross, A.J. Schultz, J.M. Williams, J. Am. Chem. Soc. 106 (1984) 5319. [20] R. Attig, J.M. Williams, Angew. Chem. Ger. Ed. 88 (1976) 507. [21] G.D. Brunton, C.G. Johanson, J. Chem. Phys. 62 (1975) 3797. [22] M.R. Spirlet, W.R. Busing, Acta Crystallogr., B 34 (1978) 907. [23] U.B. Mioc˘, Ph. Colomban, M. Davidovic´, J. Tomkinson, J. Mol. Struct. 326 (1994) 99.

[24] U.B. Mioc˘, R.Z. Dimitrijevic´, M. Davidovic´, Z.P. Nedic´, M.M. Mitrovic´, Ph. Colomban, J. Mater. Sci. 29 (1994) 3705.

[25] A. Kremenovic´, A. Spasojevic´-de Bire´, R. Dimitrijevic´, P. Sciau, U.B. Mioc˘, Ph. Colomban, Solid State Ion. 132 (2000) 39.

[26] J. Rodriguez-Carvajal, Abstracts of the Satellite Meeting on Powder Diffraction of the XV Congress of the IUCr, Toulouse, France, 1990, p. 127 (ftp://charybde.saclay.cea.fr/pub/divers).

[27] B.E. Warren, X-ray Diffraction, Addison-Wesley, Reading, MA, 1969, p. 251, Chap. 13.

[28] D. Balzar, J. Res. Natl. Inst. Stand. Technol. 98 (1993) 321.

[29] U. Mioc˘, M. Davidovic´, N. Tjapkin, Ph. Colomban, Solid State Ion. 46 (1992) 103.

[30] T. Kjaellman, I. Olovsson, Acta Crystallogr., B 28 (1972) 1692.

[31] T. Dahlems, D. Mootz, M. Schilling, Z. Naturforsch., Sec. B-A 51 (1996) 536.

[32] D. Mootz, M. Steffen, Z. Anorg. Allg. Chem. 482 (1981) 193.

[33] T. Dahlems, D. Mootz, Z. Anorg. Allg. Chem. 622 (1996) 1319.

[34] D. Mootz, E.-J. Oellers, M. Wiebcke, Acta Crystallogr., C 44 (1988) 1334.

[35] I.V. Kuzmenko, A.N. Zhilyaev, T.A. Fomina, M.A. PoraiKoshitz, I.B. Baranovskii, Z. Neorg. Khim. 34 (1989) 2548.

[36] D. Mootz, E.-J. Oellers, M. Wiebcke, Z. Anorg. Allg. Chem. 564 (1988) 17.

[37] M.S. Wickleder, Z. Anorg. Allg. Chem. 625 (1999) 474.

[38] G. Chiari, G. Ferrais, Acta Crystallogr., B 38 (1982) 2331.

[39] T. Steiner, J. Phys. Chem., A 102 (1998) 7041.

[40] G.J. Kearley, F. Fillaux, M.-H. Baron, S. Bennington, J. Tomkinson, Science 204 (1994) 1285.

[41] N. Bjerum, Science 115 (1952) 385.

[42] J.F. Nagle, in: T. Bountis (Ed.), Proton Transfer in Hydrogen Bonded Systems, Plenum, New York, 1992, p. 17.

[43] J.D. Dunitz, Nature 197 (1963) 860.

[44] N. Essayem, Y.Y. Tong, H. Jobic, J.C. Vedrine, Appl. Catal., A Gen. 194–195 (2000) 109.

[45] L. Marosi, E.E. Platero, J. Cifre, C.O. Arean, J. Mater. Chem.
10 (2000) 1949.

[46] L.J. Farrugia, J. Appl. Crystallogr. 30 (1997) 565.